Old Dominion University
ODU Digital Commons

Engineering Technology Faculty Publications | Engineering Technology

2018

Erosion Degradation Characteristics of a Linear Electro-Hydrostatic Actuator Under a High-Frequency Turbulent Flow Field

Yuan Li

Shaoping Wang

Mileta M. Tomovic
Old Dominion University, mtomovic@odu.edu

Chao Zhang

Follow this and additional works at: https://digitalcommons.odu.edu/engtech_fac_pubs

 Part of the Aerospace Engineering Commons, and the Tribology Commons

Repository Citation

Li, Yuan; Wang, Shaoping; Tomovic, Mileta M.; and Zhang, Chao, "Erosion Degradation Characteristics of a Linear Electro-Hydrostatic Actuator Under a High-Frequency Turbulent Flow Field" (2018). *Engineering Technology Faculty Publications*. 60.
https://digitalcommons.odu.edu/engtech_fac_pubs/60

Original Publication Citation

Li, Y., Wang, S. P., Tomovic, M. M., & Zhang, C. (2018). Erosion degradation characteristics of a linear electro-hydrostatic actuator under a high-frequency turbulent flow field. *Chinese Journal of Aeronautics, 31*(5), 914-926. doi:10.1016/j.cja.2017.12.002

This Article is brought to you for free and open access by the Engineering Technology at ODU Digital Commons. It has been accepted for inclusion in Engineering Technology Faculty Publications by an authorized administrator of ODU Digital Commons. For more information, please contact digitalcommons@odu.edu.

Chinese Journal of Aeronautics, (2018), 31(5): 914–926

Chinese Society of Aeronautics and Astronautics
& Beihang University

Chinese Journal of Aeronautics

cja@buaa.edu.cn
www.sciencedirect.com

Erosion degradation characteristics of a linear electro-hydrostatic actuator under a high-frequency turbulent flow field

Yuan LI [a], Shaoping WANG [a], Mileta M. TOMOVIC [b], Chao ZHANG [a,*]

[a] School of Automation Science and Electrical Engineering, Beihang University, Beijing 100083, China
[b] College of Engineering and Technology, Old Dominion University, Norfolk, VA 23529, USA

Received 31 March 2017; revised 7 July 2017; accepted 19 September 2017
Available online 8 December 2017

KEYWORDS

Computational fluid dynamics;
Degradation characteristics;
Dynamic contaminated particles concentration;
Erosion;
Linear Electro-Hydrostatic Actuator;
Performance degradation

Abstract The paper proposes a performance degradation analysis model based on dynamic erosion wear for a novel Linear Electro-Hydrostatic Actuator (LEHA). Rather than the traditional statistical methods based on degradation data, the method proposed in this paper firstly analyzes the dominant progressive failure mode of the LEHA based on the working principle and working conditions of the LEHA. The Computational Fluid Dynamics (CFD) method, combining the turbulent theory and the micro erosion principle, is used to establish an erosion model of the rectification mechanism. The erosion rates for different port openings, under a time-varying flow field, are obtained. The piecewise linearization method is applied to update the concentration of contaminated particles within the LEHA, in order to gain insight into the erosion degradation process at various stages of degradation. The main contribution of the proposed model is the application of the dynamic concentration of contamination particles in erosion analysis of Electro-Hydraulic Servo Valves (EHSVs), throttle valves, spool valves, and needle valves. The effects of system parameters and working conditions on component wear are analyzed by simulations. The results of the proposed model match the expected degradation process.

© 2017 Production and hosting by Elsevier Ltd. on behalf of Chinese Society of Aeronautics and Astronautics. This is an open access article under the CC BY-NC-ND license (http://creativecommons.org/licenses/by-nc-nd/4.0/).

1. Introduction

Integrated Electro-Hydrostatic Actuators (EHAs) have seen increased application in More-Electric Aircraft (MEA), due to their numerous advantages including high reliability, long lifetime, and high efficiency.[1–4] Traditional power-integrated Rotary Electro-Hydrostatic Actuators (REHAs) are facing many problems, such as severe heating, big inertia, low-frequency response, and difficulty in redundancy configuration. In order to solve these deficiencies, many researchers have

* Corresponding author.
E-mail address: czhangstar@gmail.com (C. ZHANG).

Peer review under responsibility of Editorial Committee of CJA.

ELSEVIER Production and hosting by Elsevier

https://doi.org/10.1016/j.cja.2017.12.002

1000-9361 © 2017 Production and hosting by Elsevier Ltd. on behalf of Chinese Society of Aeronautics and Astronautics.
This is an open access article under the CC BY-NC-ND license (http://creativecommons.org/licenses/by-nc-nd/4.0/).

proposed direct-drive EHAs.[5–9] Li et al. have presented a novel LEHA for the pump control system based on a collaborative rectification structure for linear pumps where the fundamental subsystem consists of two Direct Drive Pump Cells (DDPCs).[10] Their prototype has verified feasibility of the proposed actuator and flexibility of the dual-control strategy. Although the system has a number of advantages, its reliability characteristics, such as degradation and life prediction, need to be addressed and further improved. Applying the novel operating principle, the LEHA has improved these performance issues, but it has also introduced a problem due to the fact that it cannot integrate filters. The novel LEHA is also an integrated closed system which can increase the power-to-weight ratio. A linear resonance motor drives piston cylinder suction and discharges oil. The spool of a rectification slide valve is rigidly connected with the driving cylinder rod, resulting in the active rectification mechanism to be in a high-frequency condition. Due to non-filter design, contaminated particles will continuously cycle in an LEHA during its operation, which will precipitate further erosion and produce more contamination particles. Consequently, compared to a conventional hydraulic system with filters, the rectification mechanism in an LEHA can fail more rapidly, which can lead to a dominant progressive degradation process.

The rectification mechanism is commonly present in hydraulic systems, and when coupled with oil contamination, it can result in system failure. Some research results have indicated that contamination particles in oil wash out and wear the edges of valve components.[11] The resulting leakage increase caused by wear accounts for approximately 60% of cases of component failure. According to the research by Zhang et al., the wear resulting from particulate contaminants causes an increase in the internal leakage, the output current hysteresis and null leakage, the input current threshold, and the pressure gain, as well as a decrease in the gain linearity of the electrohydraulic servo valve.[12] The Physics-of-Failure (PoF) models of particle erosion wear introduced by Fang et al. show that the erosion wear has significant impacts on the electrohydraulic servo valve's service life and reliability.[13] Furthermore, the erosion of an LEHA is even more serious due to the particular type of motion and active rectification under relatively severe conditions. This paper is focused on the performance degradation of an LEHA induced by erosion wear.

Performance degradation analysis is extensively applied in numerous engineering fields to evaluate safety of machine parts and equipment.[14] The associated theories can be divided into three categories: (a) failure physics, (b) probability statistics, and (c) artificial intelligence. The first approach studies the structural integrity of an object with respect to operating conditions and mechanical and physical properties of materials used to make the object. Probability statistics models are mainly suitable for analysis of degradation based on stress fatigue, which requires significant amount of test data. Alternately, the artificial intelligence approach is dependent on field performance degradation data. In the field of durability analysis and life prediction, numerous physical experiments are performed in order to evaluate the life and reliability of hydraulic components. Therefore, during the design stage, it is essential to analyze the overall LEHA system based on the physical nature of erosion.

A significant number of studies have been performed to analyze the effect of erosion on system performance degradation. Fitch and Hong investigated the effects of contaminated oil on erosion in pumps and contaminant lock in servo valves, and proposed a new method to predict service life.[15] The occurrence of contaminant lock is accidental whereas the erosion caused by contaminant particulates is a continuous process which takes place as long as the system is operational. Vaughan et al. examined the effects of the particle size and concentration, differential pressure across the metering land, spool opening, spool surface, flow direction, as well as fluid characteristics on erosion wear.[16] Yang et al. adopted a gamma process to describe the internal structure degradation under erosion for electrohydraulic servo valves.[17] Zhang et al. presented a degradation assessment and life prediction method for electrohydraulic servo valves based on the CFD method and hydraulic simulation.[12] In addition, other researchers have predicted structural wear by CFD techniques.[18–20] The mechanism of erosion for a ductile metal material is a micro-cutting process, which was put forward by Finnie, who also presented an analytical erosion model to calculate erosion rates.[21] Tilly proposed that erosion of ductile materials could occur in two stages, where the first stage is micro-cutting whereas the second stage is surface fragmentation, and found that resulting estimates gave a good correlation with experimental data.[22] Recent theoretical and experimental studies explored the effects of particle properties, impacting speed and angle, and material properties on the severity of erosion. Among those studies, the Edwards model has been widely accepted to be applicable to erosion for gas-solid, liquid-solid, or gas-liquid-solid flow, where particle properties, impacting speed and angle, and material properties are taken into account.[23] Therefore, the Edwards model is utilized in this study because of its extensive applicability and high prediction accuracy. In addition, erosion due to the rectification mechanism in an LEHA under the influence of contaminant particles in hydraulic oil falls within the model framework.

This paper proposes a new method for analyzing performance degradation under dynamic erosion wear. The Edwards model is utilized to obtain erosion rates due to its broad applicability and high prediction accuracy. Furthermore, erosion rates of the rectification mechanism for different port openings and different degradation stages are estimated. In addition, in order to obtain the degradation curve under dynamic erosion wear, the concentration of contaminant particles is updated at different stages of degradation. Finally, the proposed degradation model is applied to simulate the wear degradation process in an LEHA under different flow conditions, and results are compared with results from traditional wear studies.

2. Problem description

2.1. Working principle of the LEHA

The schematic representation of the proposed LEHA architecture is shown in Fig. 1, whereas Fig. 2 represents the hydraulic circuit diagram and control loop of a traditional REHA. The REHA utilizes a motor and a pump to convert electrical energy to hydraulic energy, where the motor has reversible rotation in order to control the flow direction of hydraulic oil. Compared with the REHA, the proposed LEHA has the following distinct characteristics: (1) a linear resonance motor

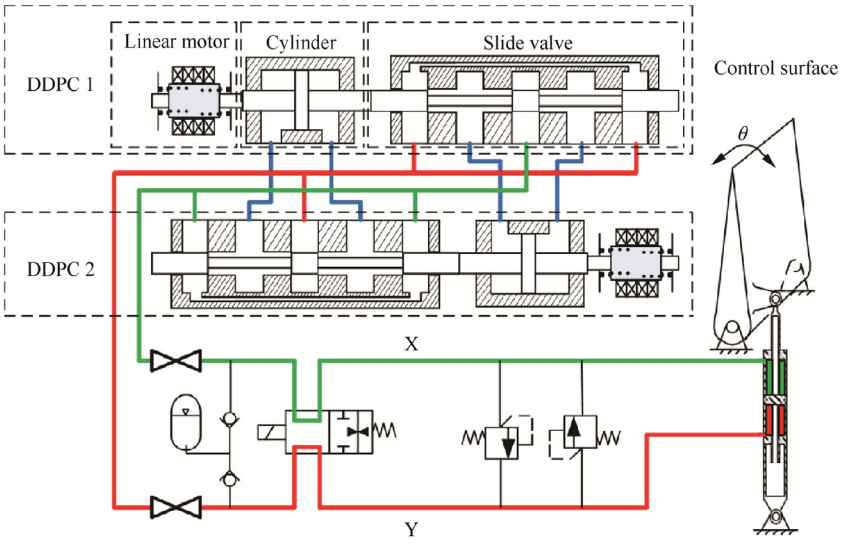

Fig. 1 Hydraulic circuit diagram of the novel LEHA design.

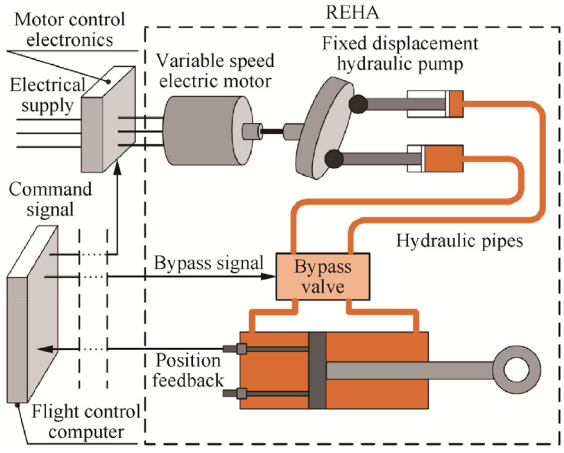

Fig. 2 Functional diagram and control loop of an REHA.

corresponding to the rotating electric machine, (2) a single direct drive piston cylinder corresponding to the traditional rotary piston pump, (3) a rectification model with passive reliance on a valve plate and active collaborative rectification dependence on a three-position four-way slide valve, and (4) direction control achieved through the phase difference between two DDPCs. The linear motor commonly operates in the resonant working mode in order to generate the maximum energy output. A Direct Drive Pump Module (DDPM) consists of DDPC1 and DDPC2, which are characterized with collaborative rectification. A DDPC consists of a cylinder and a valve, where a piston rod and a valve spool are integrated, and is driven directly by the linear resonating motor. X and Y are the interface ports of the DDPCs: one is the inlet and the other is the outlet. The deflection angle of aircraft's control surface is θ. As a result, the novel pump is more compact and has better controllability. The theoretical research and experimental results conducted on the prototype valve have demonstrated that the DDPC-discharged kinematic flow volume depends on the phase difference between the two cells. The output flow in one cycle from a DDPM port is represented by

$$V = -8A_c S_p \sin\varphi \tag{1}$$

where V is the output flow in one cycle from a DDPM port, A_c is the piston's effective area, S_p is the resonance amplitude of a DDPC, and φ is the phase difference between the two cells.

The kinematic volume efficiency is maximum for $\varphi = \pm\pi/2$, and zero for $\varphi = 0$ or $\varphi = \pm\pi$.

2.2. Dominant mode of gradual failure

At an earlier stage, a Failure Mode and Effect Analysis (FMEA) was performed for the LEHA.[24] The results show that resonant spring fatigue damage and rectification mechanism erosion are the two major progressive failure modes affecting the performance of the LEHA. The LEHA failure is defined as a condition when a performance indicator cannot be maintained within a specified range. The effect of rectification mechanism erosion is shown in Fig. 3, where P, T, A, and B are the hydraulic oil ports of the three-position four-way valve. The figure indicates possible fluid flow patterns in the rectification slide valve when port P is connected with X and port T is connected with Y. It can be seen that the rectification valve is characterized by reciprocating flushing which is different from single-direction flushing which occurs in a traditional valve. The rectification valve at the middle position is equivalent to a piston pump at the upper or lower dead point. Consequently, wear of the internal structure can cause an increase in internal leakage and result in power loss.

The major sources of initial contamination include particulates resulting from the manufacturing process, dust inclusions from storage, and contaminant particles mixed in oil. These contaminants can impact the system in three different ways: (a) three-body abrasion, (b) particle impingement erosion, and (c) motion impediment.[15] Motion impediment is rare in practice and caused by relatively large particles. However, the erosion problem is common, and can become serious as the process has a tendency of having positive feedback.

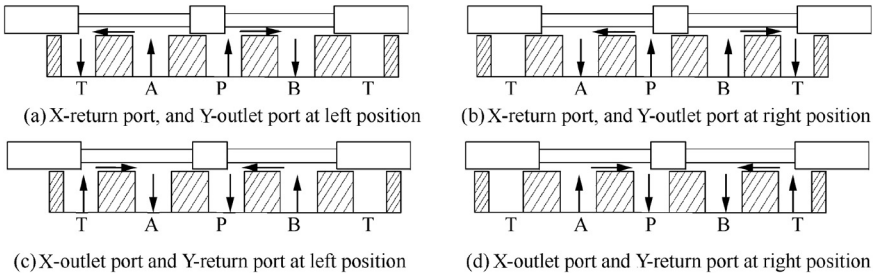

Fig. 3 Fluid flow in the rectification slide valve when P is connected with X and T is connected with Y.

The major impact of erosion is reflected on the performance of the LEHA. Namely, there are two ways in which the power/weight ratio of the LEHA can be affected: one is a change in the resonant frequency and the other one is a change in the amplitude. The resonant amplitude is subject to the size of the DDPM, which makes modification in the frequency become the most effective method. The initial clearance between the valve spool and sleeve in new valves is generally in the range of 3–5 μm, and the corner radius of edges is generally below 0.5 μm. Throughout their lifecycles, valves will undergo erosion which will cause an increase in internal leakage, which, on the other hand, will ultimately degrade the system performance.

3. Mathematical model of the degradation process

The erosion-induced performance degradation process can be analyzed in three consecutive steps: (1) identification of the potential erosion location and determination of the fluid dynamic boundary, (2) determination of the structural degradation after erosion, and (3) prediction of the erosion rate.

3.1. Stress-strain equation of the dynamic boundary

The erosion wear is analyzed in both valve and piston regions as indicated in Fig. 4. P_{v1}, T_{v1}, A_{v1}, and B_{v1} are the hydraulic oil ports of the valve in DDPC1. A_{p2} and B_{p2} are the cylinder chambers in DDPC2. The displacement of the mover is x_1 in DDPC1, and the velocity is v_1. Similarly, the displacement of the mover is x_2 in DDPC2, and the velocity is v_2. The positive direction is the cylinder pointing to the valve. When the spool in DDPC1 or DDPC2 is at the zero displacement, i.e., $x_1 = 0$ or $x_2 = 0$, there is no connection between P, T and A, B. The piston determines the flow velocity and flow rate through the valve inlet, and in turn, the valve transfers the load pressure to the piston.

The continuity equations of hydraulic chambers A_{p2} and B_{p2} can be written as

$$\frac{dP_{dA2}}{dt} = -\frac{\beta_e}{V_{dA2}}[q_{dA2out} + C_{ip}(P_{dA2} - P_{dB2}) + C_{ep}P_{dA2} - A_c\dot{x}_2] \tag{2}$$

$$\frac{dP_{dB2}}{dt} = \frac{\beta_e}{V_{dB2}}[q_{dB2in} + C_{ip}(P_{dA2} - P_{dB2}) - C_{ep}P_{dB2} - A_c\dot{x}_2] \tag{3}$$

$$V_{dA2} = V_{dA02} + A_c x_2 \tag{4}$$

$$V_{dB2} = V_{dB02} - A_c x_2 \tag{5}$$

where P_{dA2} is the hydraulic pressure in the left chamber, P_{dB2} is the hydraulic pressure in the right chamber, β_e is the effective bulk modulus (including hydraulic oil, connecting pipes, and the cylinder's mechanical flexibility), V_{dA2} is the volume of the left chamber (including valves and connecting pipes), V_{dB2} is the volume of the right chamber (including valves and connecting pipes), C_{ip} is the cylinder's internal leakage coefficient, C_{ep} is the cylinder's external leakage coefficient, q_{dA2out} is the outflow from the cylinder's left chamber, q_{dB2in}

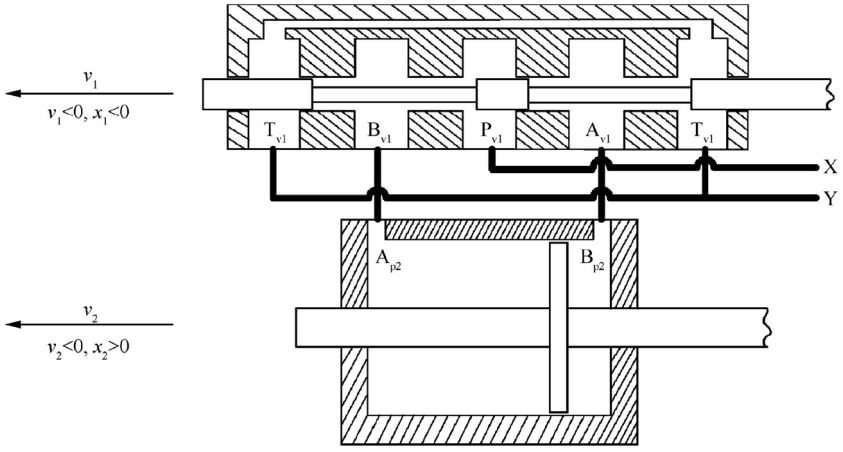

Fig. 4 Schematic diagram of the reciprocating system.

is the inflow to the cylinder's right chamber, V_{dA02} is the initial volume of the left chamber, and V_{dB02} is the initial volume of the right chamber.

The fluid flow rate Q from the driven hydraulic cylinder chamber to the valve entrance can be described by the following orifice flow equation:

$$Q = C_d A_e \sqrt{\frac{2(P_f - P_b)}{\rho}} \tag{6}$$

$$Q = v_{pa} A_p \tag{7}$$

where C_d is the flow coefficient of the orifice, A_e is the effective area of the orifice, P_f is the hydraulic pressure in front of the orifice, P_b is the hydraulic pressure behind the orifice, ρ is the fluid density, v_{pa} is the average velocity of fluid at the valve inlet, and A_p is the cross-sectional area of the valve inlet.

3.2. Continuous flow model

The continuous phase modeling uses Reynolds averaged Navier-Stokes equations. Because of enhanced accuracy for rapidly strained and swirling flows, the RNG k-ε model is selected for turbulence, where the continuity equation is described as

$$\nabla \times (\rho \boldsymbol{v}) = 0 \tag{8}$$

where $\boldsymbol{v}$ is the velocity of fluid.

3.3. Structural degradation model

According to a significant number of published results, erosion has the greatest impacts on the radial clearance between the spool and the sleeve, and on the throttle edge radii. An ideal geometry calls for the throttle edges to be perfectly square with no rounding.[11–13,25,26] The erosion process will cause the throttle edges to wear and develop radii, resulting in an increase of the radial clearance between the spool and the sleeve, as shown in Fig. 5. The radial clearance between the spool and the sleeve has a small initial value because of the fluid's lubrication.

According to the Pythagorean theorem, the gap between the spool and the sleeve can be determined as

$$\delta_2 = \sqrt{(\delta_1 + r_1 + r_2)^2 + (r_1 + r_2)^2} - (r_1 + r_2) \tag{9}$$

where δ_1 is the radial clearance between the spool and the sleeve, δ_2 is the flow clearance between the spool and the sleeve, r_1 is the radius of the spool's throttle edge, r_2 is the radius of the sleeve's throttle edge.

It is assumed that $r = r_1 = r_2$, since the difference between r_1 and r_2 is relatively small.

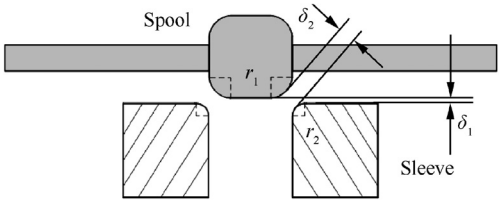

Fig. 5 Throttle edge after wear.

3.4. Wear volume model

The geometry of the cylindrical spool changes during erosion wear as indicated in Fig. 6. Assuming the same wear conditions between contact surfaces, then the degrees of wear of the spool and the sleeve can be assumed to be equal. In addition, it is assumed that the wear rate of each orifice is the same. Since the edge radius, r, is small compared to the spool radius, R_s, the radius of the spool, R_s, is considered to remain constant throughout the process.

The longitudinal cross section of the wear-free spool is assumed to be rectangular with square edges. As wear progresses, the spool edges start to develop a quarter-round geometry of radius r. The total wear volume of a valve's orifice can be obtained by the following equation:

$$V_o = 2V_s = 2\left(1 - \frac{\pi}{4}\right) r^2 c = 0.4292 r^2 \tag{10}$$

$$c = 2\pi R_s \tag{11}$$

where V_o is the total wear volume of a valve's orifice, V_s is the wear volume of a single throttle edge, r is the equivalent radius of the throttling edge, c is the perimeter of the throttle edge, and R_s is the radius of the spool's boss.

The total wear volume of the valve can be obtained by the time integration of the erosion wear rate as follows:

$$6 V_o \rho_p = s_e \int_0^t \rho_e(t) \mathrm{d}t \tag{12}$$

where ρ_p is the contaminated particle's density, s_e is the eroded area, and $\rho_e(t)$ is the erosion rate function.

3.5. Contaminant particle concentration model

During a lifetime of LEHA operation, metal particles generated by wear end up in hydraulic oil. Since the LEHA is a closed system, it is reasonable to assume that all particles produced by wear are accumulated in the working hydraulic oil. The contaminant particulate concentration can be expressed by the following mass conservation equation:

$$\frac{\eta_0}{Q} V_h + 12 \rho_p V_o = \frac{\eta}{Q} V_h \tag{13}$$

where η_0 is the initial particle mass flow rate, η is the particle mass flow rate with the corresponding wear volume V_o, and V_h is the hydraulic oil volume in the LEHA.

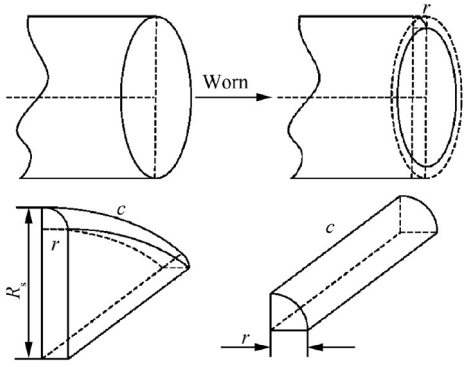

Fig. 6 Geometries of worn throttle edges.

3.6. Discrete phase model

The dynamics equation of a particle in a Lagrangian reference frame can be expressed as

$$\frac{\mathrm{d}u_\mathrm{p}}{\mathrm{d}t} = F_\mathrm{D}(\boldsymbol{u}-\boldsymbol{u}_\mathrm{p}) + \frac{\boldsymbol{g}(\rho_\mathrm{p}-\rho)}{\rho_\mathrm{p}} + \boldsymbol{F}_x \tag{14}$$

where $\boldsymbol{u}$ is the fluid velocity, $\boldsymbol{u}_\mathbf{p}$ is the particle velocity, and u_p is the scalar form of the particle velocity. $F_\mathrm{D}(\boldsymbol{u}-\boldsymbol{u}_\mathbf{p})$ represents the force load on unit particle mass, $\boldsymbol{g}$ is the acceleration of gravity, and $\boldsymbol{F}_x$ is the additional force including Saffman's lift force, the virtual mass force, the pressure gradient force, the thermophoretic force, the forces in moving reference frames, and the Brownian Force.

$$F_\mathrm{D} = \frac{18\mu}{\rho_\mathrm{p} d_\mathrm{p}^2}\cdot\frac{C_D Re}{24} \tag{15}$$

$$Re = \frac{\rho d_\mathrm{p}\left|\boldsymbol{u}_\mathrm{p}-\boldsymbol{u}\right|}{\mu} \tag{16}$$

where d_p is the particle's diameter, Re is the relative Reynolds number, μ is the dynamic viscosity of the fluid, and C_D is the drag coefficient, which is defined by Haider and Levenspiel[27] as

$$C_D = \frac{24}{Re}\left(1+b_1 Re^{b_2}\right) + \frac{b_3 Re}{b_4+Re} \tag{17}$$

$$\begin{cases} b_1 = \exp(2.3288 - 6.4581\Phi + 2.4486\Phi^2) \\ b_2 = 0.0964 + 0.5565\Phi \\ b_3 = \exp(4.905 - 13.8944\Phi + 18.4222\Phi^2 - 10.2599\Phi^3) \\ b_4 = \exp(1.4681 + 12.2584\Phi - 20.7322\Phi^2 + 15.8855\Phi^3) \end{cases} \tag{18}$$

$$\Phi = \frac{s}{S} \tag{19}$$

where Φ is the particle shape factor, s is the surface area of a sphere with the same volume as the particle, and S is the actual surface area of the particle, and b_1, b_2, b_3, and b_4 are coefficients related to Φ.

It can be assumed that the particle volume fraction or concentration is very low and that the collision between particles can be neglected.

3.7. Particle-wall collision-rebound model

When particles impinge the valve wall at a certain angle and speed, they rebound at a certain angle and speed, as shown in Fig. 7. The energy loss during collision can be determined from the impulse-momentum principle where normal and tangential restitution coefficients are employed, which are introduced as

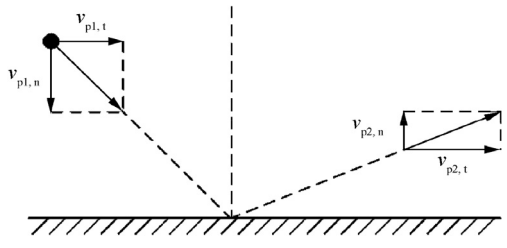

Fig. 7 Schematic diagram of particle-to-wall collision-rebound.

$$\varepsilon_\mathrm{N} = \frac{v_{\mathrm{p2,n}}}{v_{\mathrm{p1,n}}} \tag{20}$$

$$\varepsilon_\mathrm{T} = \frac{v_{\mathrm{p2,t}}}{v_{\mathrm{p1,t}}} \tag{21}$$

where ε_N is the normal restitution coefficient, ε_T is the tangential restitution coefficient, $v_{\mathrm{p1,n}}$ and $v_{\mathrm{p1,t}}$ are the particle's normal and tangential velocities with respect to the wall prior to collision, and $v_{\mathrm{p2,n}}$ and $v_{\mathrm{p2,t}}$ are the particle's normal and tangential velocities after collision.

It has been demonstrated by Grant and Forder et al. that restitution coefficients are dependent on the particle impingement angle, α_p.[28,29] Furthermore, Forder et al. provided the expressions of restitution coefficients as follows:

$$\varepsilon_\mathrm{N} = 0.988 - 0.78\alpha_\mathrm{p} + 0.19\alpha_\mathrm{p}^2 - 0.024\alpha_\mathrm{p}^3 + 0.027\alpha_\mathrm{p}^4 \tag{22}$$

$$\varepsilon_\mathrm{T} = 1 - 0.78\alpha_\mathrm{p} + 0.84\alpha_\mathrm{p}^2 - 0.21\alpha_\mathrm{p}^3 + 0.028\alpha_\mathrm{p}^4 - 0.022\alpha_\mathrm{p}^5 \tag{23}$$

3.8. Semi-empirical material removal model

The Edwards model is commonly used to determine the erosion rate for certain particle concentration and wall boundaries, and can be expressed as follows:

$$R_\mathrm{erosion} = \sum_{p=1}^{N_\mathrm{p}} \frac{m_\mathrm{p} C(d_\mathrm{p}) f(\alpha_\mathrm{p}) v_\mathrm{p}^{b(v_\mathrm{p})}}{A_\mathrm{face}} \tag{24}$$

where N_p is the number of particles that impact the area represented by A_face, m_p is a particle's mass, $C\,(d_\mathrm{p})$ is the function of a particle's diameter, v_p is the particle velocity relative to the wall, $b(v_\mathrm{p})$ is the function of the relative particle velocity, A_face is the area of the cell face on the wall, and $f\,(\alpha_\mathrm{p})$ is the function of the impact angle, which is determined as

$$f(\alpha_\mathrm{p}) = \begin{cases} 0.04\alpha_\mathrm{p} & 0 \le \alpha_\mathrm{p} < 20^\circ \\ 0.02\alpha_\mathrm{p} + 0.4 & 20^\circ \le \alpha_\mathrm{p} < 30^\circ \\ -\frac{1}{30}\alpha_\mathrm{p} + 2 & 30^\circ \le \alpha_\mathrm{p} < 45^\circ \\ -\frac{1}{450}\alpha_\mathrm{p} + 0.6 & 45^\circ \le \alpha_\mathrm{p} \le 90^\circ \end{cases} \tag{25}$$

4. Simulation of erosion wear

A well-established three-step erosion prediction approach using the Eulerian-Lagrangian approach is used in this work to simulate the process. The model, which has been adopted by many authors, consists of the following steps: (1) flow field prediction using viscous or inviscid models, (2) particle trajectory calculation by modeling discrete particle dynamics, and (3) determination of erosion wear using a material removal model. The development of the Eulerian-Lagrangian model of fluid particle flows is well documented and will not be discussed in detail. However, certain aspects of the erosion model applied in this study are discussed below.

The model of fluid flow is based on the Reynolds averaged Navier-Stokes equations, while the RNG k-ε model, due to its enhanced accuracy for rapidly strained and swirling flows, is

used to describe turbulence. The particle trajectory and its velocity are determined by solving a set of ordinary differential equations formed by the Lagrangian method. A simulation is performed with ANSYS Workbench 15.0.

The simulation is based on the implementation of the flow chart shown in Fig. 8. Firstly, the spool position and the concentration of contaminant particles are determined. A dimensional fluid domain model is established next, followed by meshing, parameter initialization, and calculation of erosion wear. The erosion wear is recalculated when the spool position or contaminated particles' concentration changes. Finally, an erosion degradation curve is obtained by integrating the erosion rate with respect to time.

The main structural parameters of the LEHA's rectification mechanism are given in Table 1. The initial flow rate of hydraulic oil with contaminant particles can be obtained by 7th level.[12] It is assumed that the particles are pure iron, the reciprocating frequency is 100 Hz, and the opening size is ± 3 mm. The dynamic fluid boundary conditions can be obtained from Eqs. (7) and (8). In order to achieve high computational effectiveness, an optimal algorithm is used to balance the grid quality and calculation time. The resulting computational domain mesh is shown in Fig. 9. The standard case simulation parameters are given in Table 2.

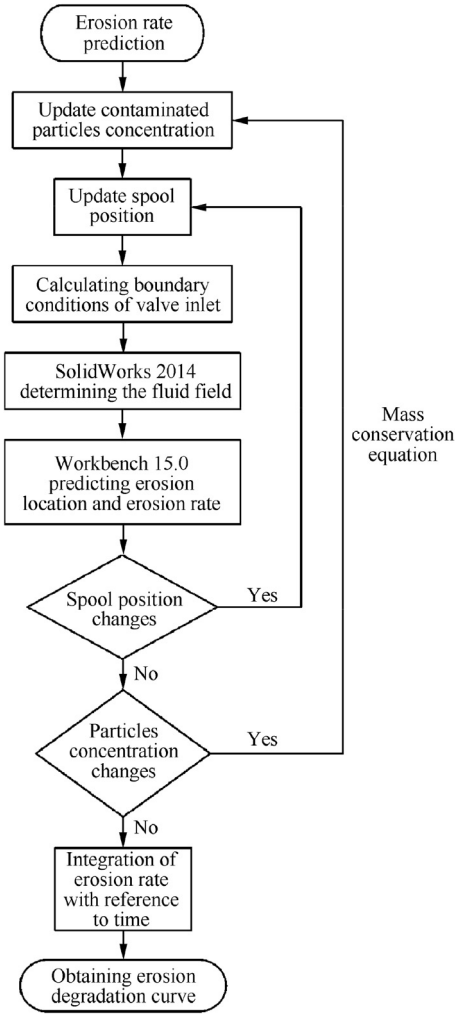

Fig. 8 Algorithm for erosion prediction.

Table 1 Main structural parameters of the LEHA.

Structural parameters		Value
Diameter spool	d_{sp}	7 mm
Diameter cylinder's rod	d_{cr}	7 mm
Diameter cylinder's piston	d_{cp}	10.5 mm
Valve stroke	S_v	3 mm
Diameter hydraulic pipe	d_p	3 mm
Hydraulic oil volume	V_h	0.5 L

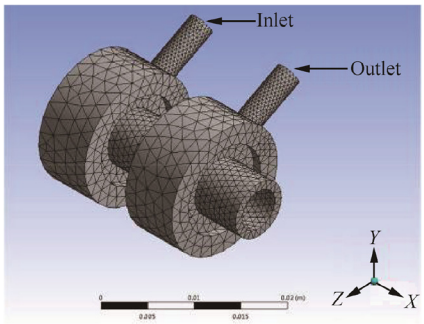

Fig. 9 Computational domain and mesh (when the valve opening is 50%).

In addition, the conventional SIMPLE algorithm is applied to couple pressure and velocity via a second-order upwind scheme for the momentum. The convergence criterion is set so that the residual is smaller than 10^{-3}.

The simulation results representing the erosion rate contours of the spool valve are shown in Fig. 10. The results indicate that the edge of the throttle orifice is experiencing the most serious erosion. The results are consistent with the published results focused on erosion of EHSVs, throttle valves, and needle valves.[11–13,17,25,30,31] The particle path lines and associated velocity magnitudes are shown in Fig. 11. The areas with high-speed profiles are evident in the orifice edge region, where the particle velocity can be in excess of 100 m/s. Having a large number of particles with significant kinetic energy, directly impinging the orifice, will result in a severe erosion of the surface.

5. Results and discussion

5.1. Effect of the opening gap on the erosion rate

The average erosion rate of a sharp edge as a function of the valve opening (d_{op}), during the early stage of degradation, is shown in Fig. 12. Correspondingly, Fig. 13 depicts the erosion rate distribution in the throttling edge for different valve opening sizes. The results are for valve port opening between 0 mm and 3 mm. It can be observed that the maximum average erosion rate occurs when the EHSV opening is 0.5 mm, and that the average erosion rate decreases rapidly for opening sizes between 0.5 mm and 1.0 mm.

Table 2 Standard case simulation parameters.

Case	Valve opening	Inlet velocity	Inlet pipe diameter	Load pressure	Particle concentration	Particle diameter
Standard	0.5 mm	55 m/s	3.0 mm	3 MPa	1.78×10^{-7} kg/s	5 μm

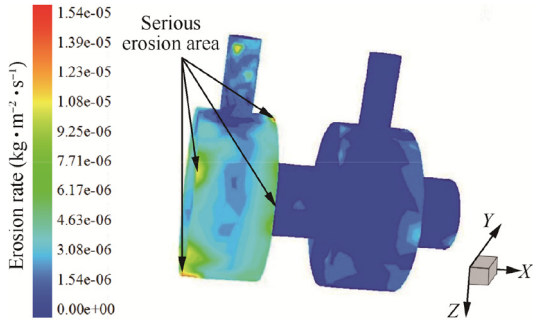

Fig. 10 Erosion rate contours of the valve.

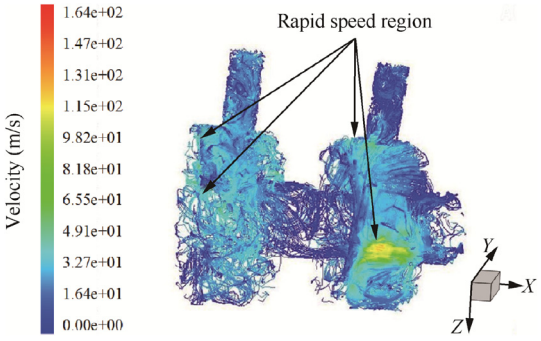

Fig. 11 Particles' path lines of the velocity magnitude.

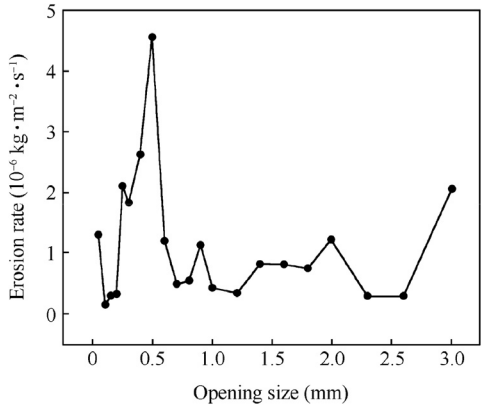

Fig. 12 Erosion wear rate under different valve opening sizes.

5.2. Effect of the inlet velocity on the erosion rate

In this section, the effect of the inlet velocity (v_{in}) on flow erosion is studied. Simulations are performed for different inlet velocities while keeping other parameters the same as those in the standard case. The erosion rate distribution in the throttling edge as a function of the inlet velocity is shown in Fig. 14.

It is apparent that an increase in the inlet velocity increases the erosion severity of both the sleeve and the spool. It is also apparent that the erosion is maximum at the maximum-velocity locations, which occurs at the gap between the edges of the valve spool and sleeve. The simulation results indicate that the erosion zone on the spool wall increases simultaneously with an increase in the severity of erosion as the inlet velocity increases from 45 m/s to 65 m/s, while the erosion in the sleeve is consistently spread over the entire throttle side.

The maximum erosion rate on the spool occurs at an inlet velocity of 65 m/s and is about 8.9 times higher than that at an inlet velocity of 45 m/s, while the maximum erosion rate along the sleeve throttle side for an inlet velocity of 65 m/s is 6.1 times higher than that for an inlet velocity of 45 m/s.

5.3. Effect of the inlet pipe diameter on the erosion rate

The erosion rates for different inlet pipe diameters but for constant pressure and opening are shown in Fig. 15. It can be observed that the maximum erosion wear rate initially increases and then decreases with an increase of the inlet diameter. The magnitude of the maximum erosion rate, for both the spool and the sleeve, is largest at $d_{in} = 4$ mm. The erosion rate of the valve spool for an inlet pipe diameter of $d_{in} = 2.5$ mm is approximately 8%, whereas for $d_{in} = 4$ mm, it is 7.5%.

The results indicate that increasing the diameter of the inlet pipe results in an increase of the flow through the gap between the spool and the sleeve, which ultimately leads to an increase in the erosion severity.

5.4. Effect of the load pressure on the erosion rate

The results indicating the erosion rate distribution on the valve spool and along the sleeve for different levels of load pressure (P_l) are shown in Fig. 16. When the load pressure increases from 0 MPa to 5 MPa, the erosion wear rate decreases slowly, whereas the erosion rate decreases rapidly with the load pressure increasing from 5 MPa to 8 MPa. The maximum erosion rates on the spool and along the sleeve throttling edges for a load pressure of 0 MPa are respectively 3.21 times and 3.46 times higher than those for a load pressure of 5 MPa. The erosion rate decreases rapidly when the load pressure increases to 8 MPa.

A lower load pressure causes a greater pressure drop on the valve path, resulting in a greater velocity of particles impinging on the valve wall, which increases erosion wear.

5.5. Effect of the particle concentration on the erosion rate

The results indicate that the particle concentration (c_p), expressed as the particle mass flow rate, plays a significant role in affecting the erosion, as shown in Fig. 17. In addition, increasing the particle mass flow rate results in an increase of the erosion-dominated zone as well as the severity of erosion.

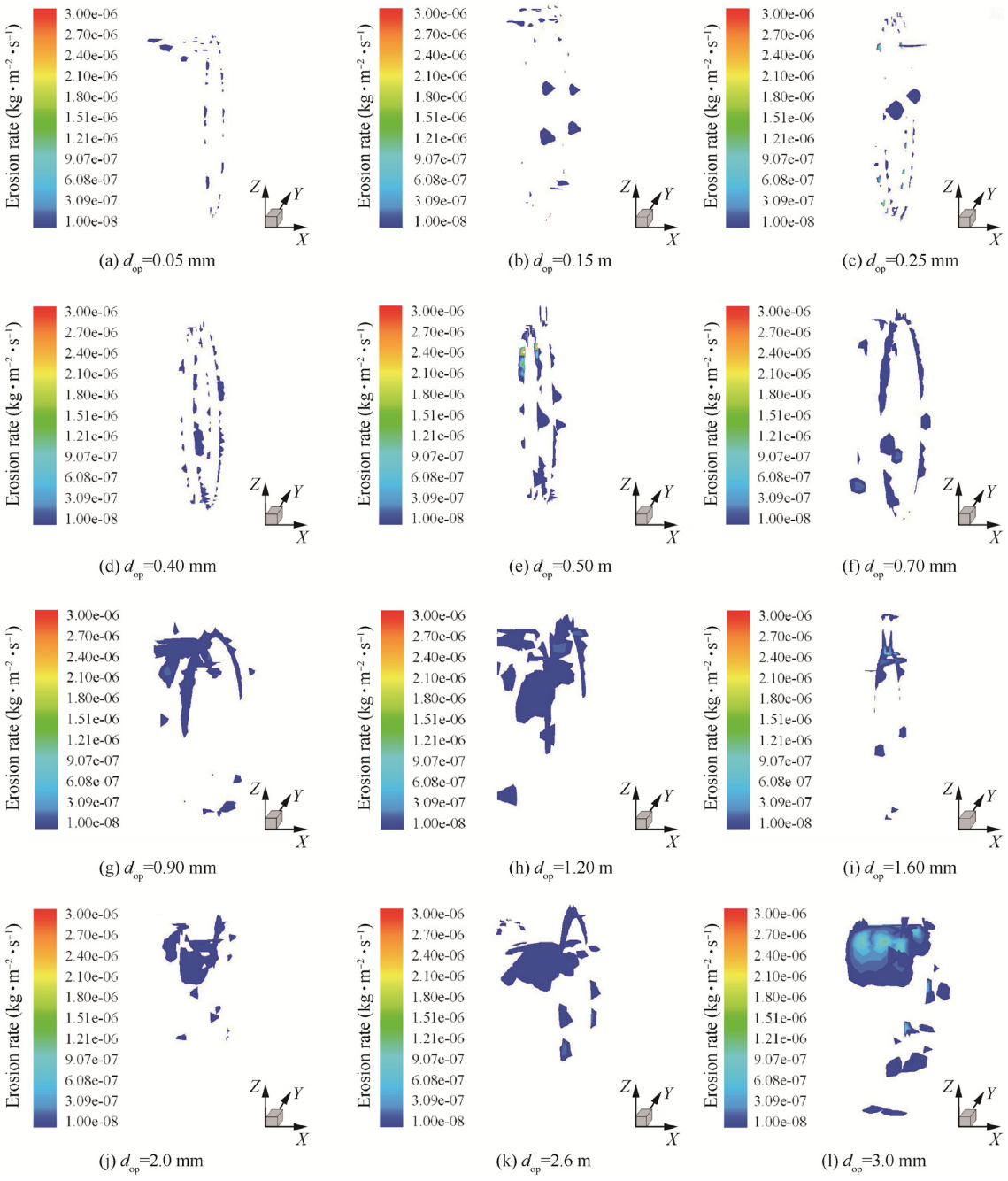

Fig. 13 Erosion rate distribution in the throttling edge under different valve opening sizes.

As the mass flow rate increases from 1.78×10^{-7} kg/s to 3.56×10^{-7} kg/s, the erosion zone extends to the entire throttling edge. The peak erosion rate of the spool at a particle mass flow rate of 3.56×10^{-7} kg/s is approximately 2.64 times of that at a flow rate of 1.78×10^{-7} kg/s. Whereas, the maximum erosion rate along the sleeve at a particle mass flow rate of 3.56×10^{-7} kg/s is about 2.21 times of that at a flow rate of 1.78×10^{-7} kg/s.

The higher the particle mass flow rate is, the more particles impinge on the spool and the sleeve per unit time. The result is that the same region is impacted by a larger number of particles.

5.6. Effect of the particle diameter on the erosion rate

The results indicate that the particle diameter clearly affects the erosion rates of both the spool and the sleeve, as illustrated in Fig. 18. As the particle diameter increases from 1 μm to 3 μm, the erosion rate increases rapidly; however, as the particle diameter increases from 3 μm to 20 μm, the erosion rate decreases slowly. The maximum erosion rates of the spool and along the sleeve at a particle diameter of 3 μm are respectively 2.41 and 2.35 times higher than those for a particle diameter of 1 μm. Furthermore, the maximum erosion rates of the spool and along the sleeve for a particle diameter of 3 μm

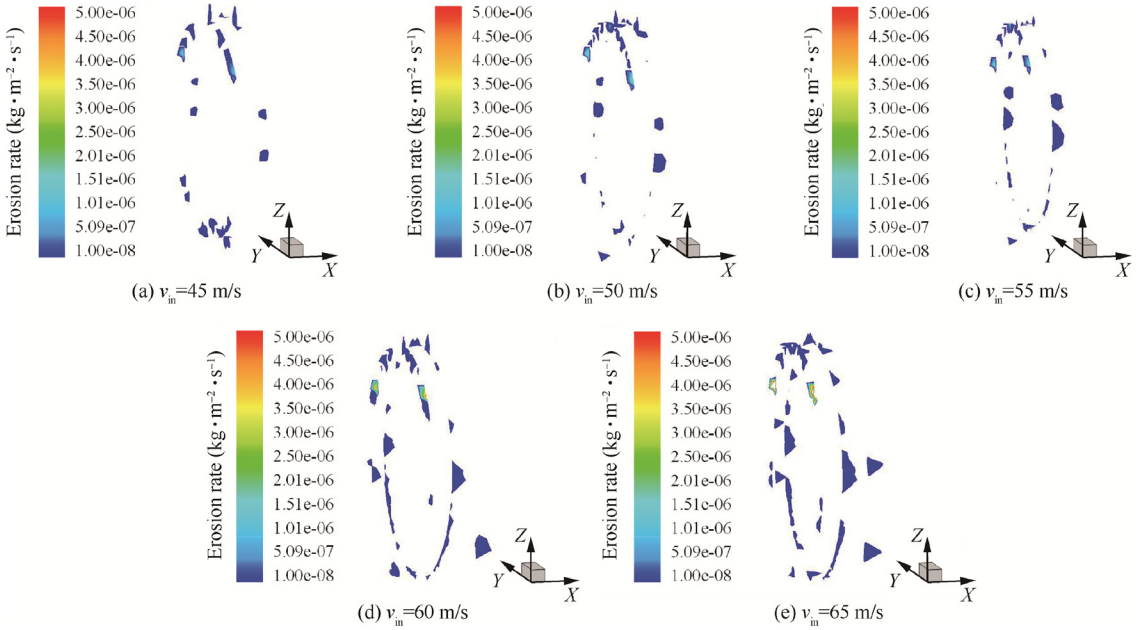

Fig. 14 Erosion rate distribution in the throttling edge under different inlet velocities.

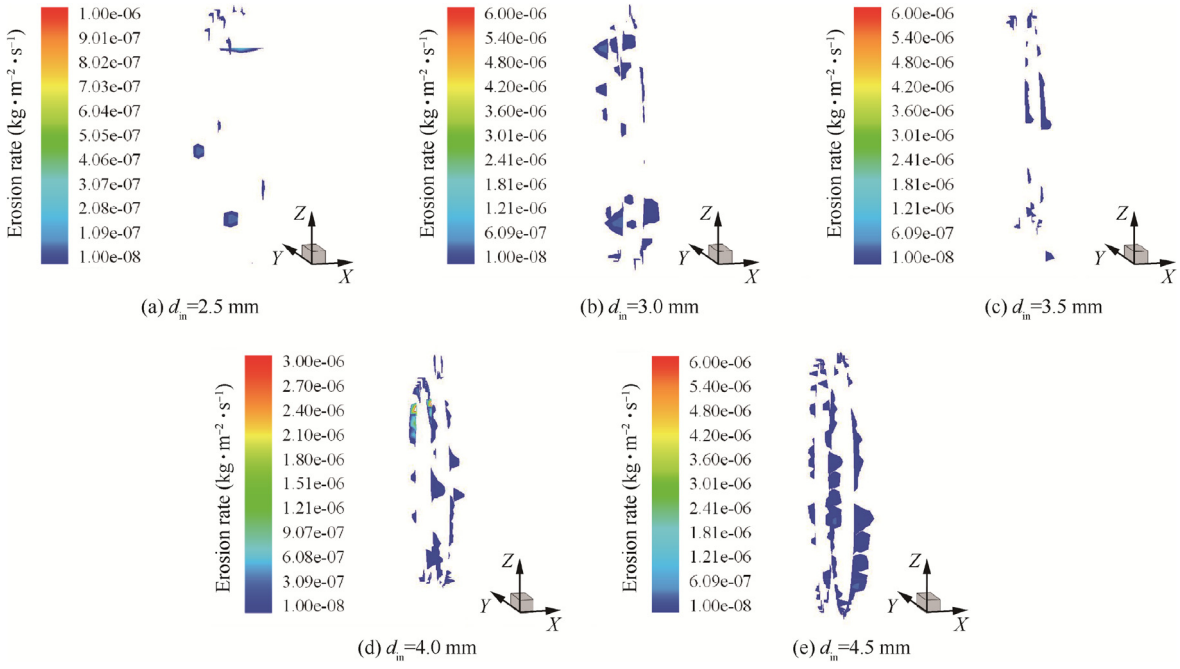

Fig. 15 Erosion rate distribution in the throttling edge under different inlet pipe diameters.

are respectively 16.23 and 15.64 times of those for a particle diameter of 15 μm. The results indicate that the particle diameter has a significant effect on erosion.

The underlying assumption is that the mass flow rate of particles is constant. Consequently, the larger the diameter of a single particle, the greater the mass of a single particle, and the smaller the number of particles. When the number of particles in the unit volume decreases, the probability of the particles impacting the spool or the sleeve is reduced with the number of particles passing through the gap between the valve spool and the sleeve. For the same velocity, a particle of a larger mass has greater kinetic energy than that of a particle of a smaller mass. As a result, assuming the same incidence angle, a particle of a larger mass causes more severe erosion than a particle of a smaller mass. As the particle diameter increases from 1 μm to 3 μm, the particle inertial force

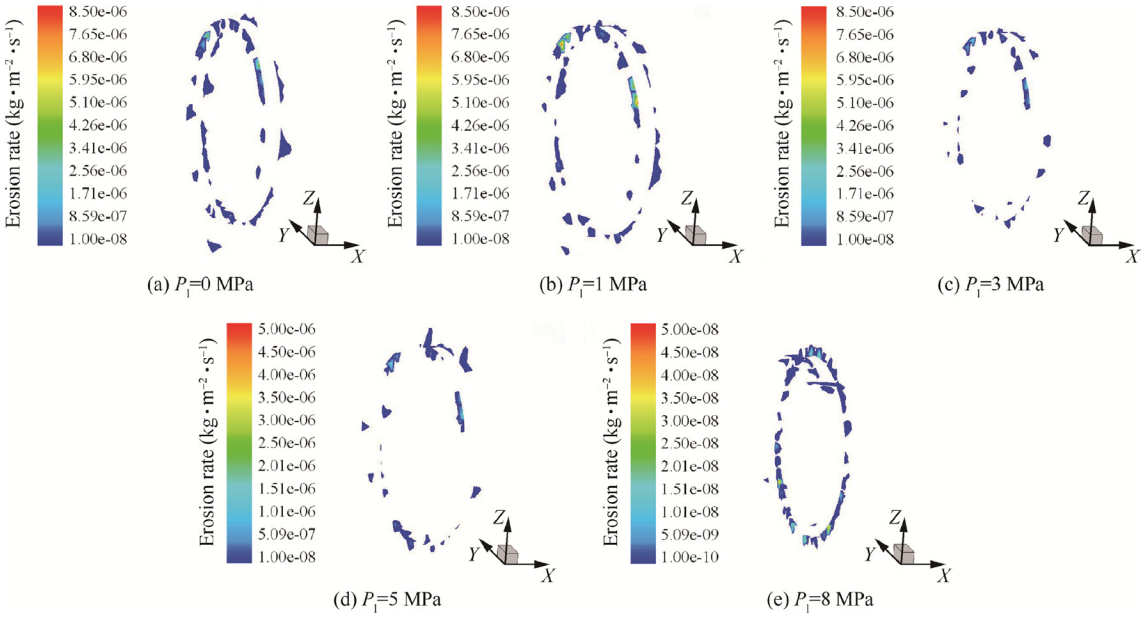

Fig. 16 Erosion rate distribution in the throttling edge under different load pressures.

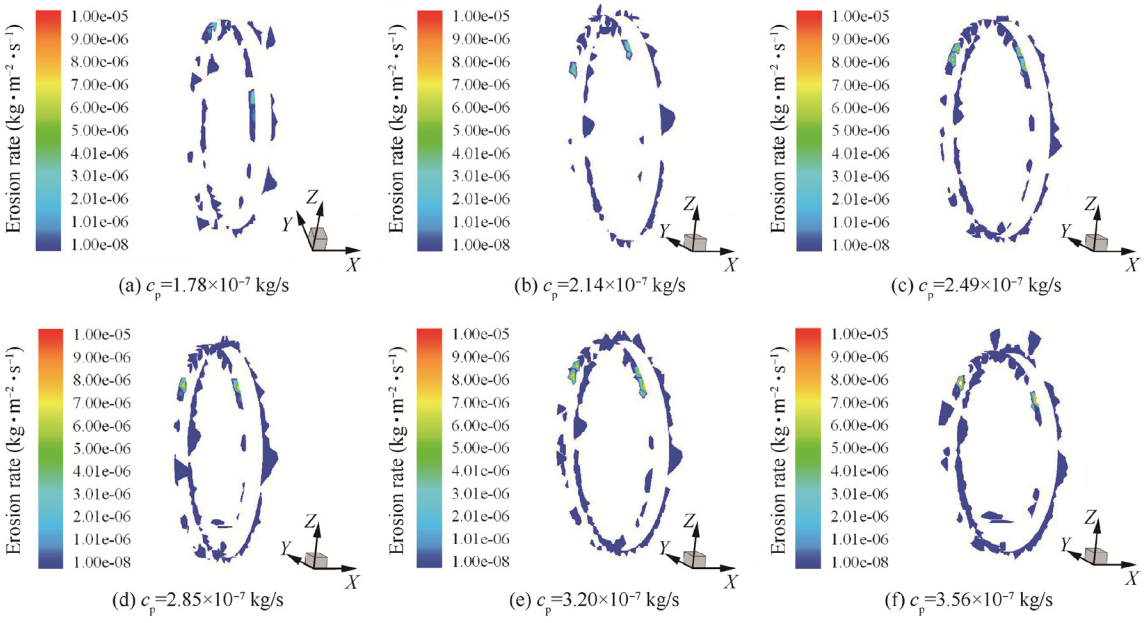

Fig. 17 Erosion rate distribution in the throttling edge under different particle concentrations.

plays a dominant role in the erosion process, while for particle sizes between 3 μm and 15 μm, the number of particles plays a primary role.

6. Conclusions

The paper introduces the working principle of a novel LEHA design, which is an integrated closed system without filters. A study was performed to analyze the effects of contaminant particles, caused by the system erosion wear, on the internal leakage of the valve and ultimately on its performance. According to failure analysis, erosion is the dominant progressive failure mode of the LEHA. Since the system does not include filters, the mass of contaminant particles accumulates over the life of the valve, which can lead to progressive failure of the system. Simulation results provide insight into the effects of valve opening on the erosion rate and the relationship between the erosion rate and structural degradation. A comparison between the simulation results and published wear erosion results for EHSVs indicates that the proposed analysis approach is effective. The following conclusions can be made based on the simulation results: (1) the erosion wear dominates the service life of the LEHA (not considering accidental failure), (2) the throttle edge erodes fastest, caused by dissipation

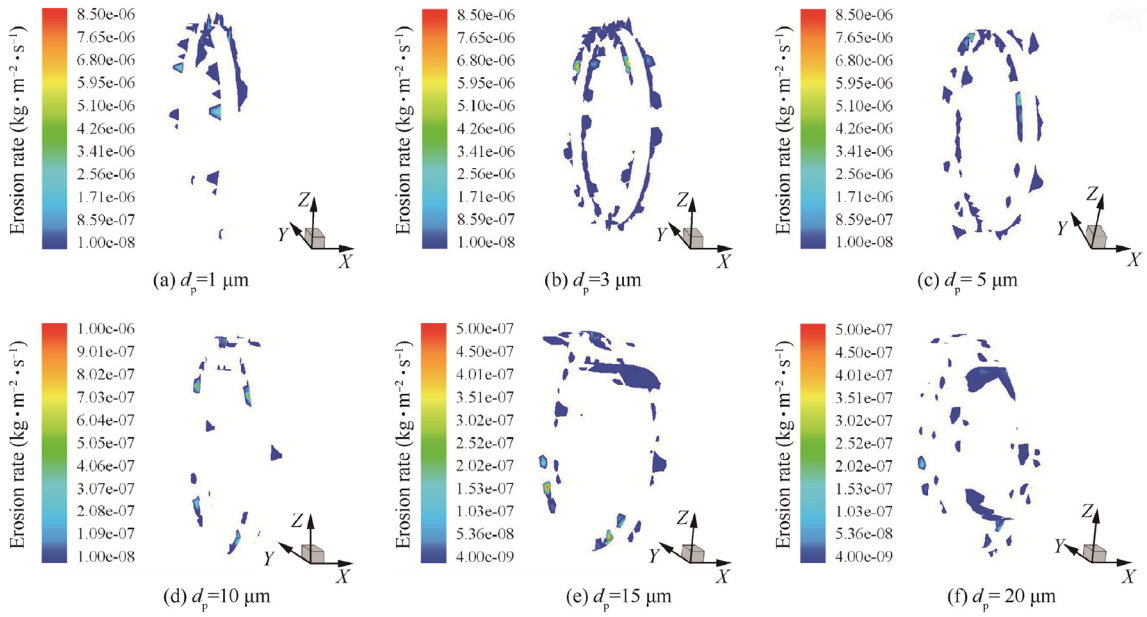

Fig. 18 Erosion rate distribution in the throttling edge under different particle diameters.

of the kinetic energy of a large number of high-speed particles at that location, and (3) the erosion of the LEHA is an accelerated degradation process. The proposed approach can be used to evaluate the service life of the LEHA and to further guide the design of the LEHA's rectification valve structure.

An experimental setup is under construction, which will provide verification of the proposed analysis model, and enable further studies of erosion phenomena in the LEHA and their effects on performance degradation of the LEHA.

Acknowledgements

This work was supported by the National Natural Science Foundation of China (Nos. 51620105010, 51675019, 51575019), the National Basic Research Program of China (No. 2014CB046402), and the Program 111 of China. The authors would also like to thank the reviewers and the editor for their comments and suggestions that led to significant improvement in the quality of the paper.

Appendix A. Supplementary material

Supplementary data associated with this article can be found, in the online version, at https://doi.org/10.1016/j.cja.2017.12.002.

References

1. Van den Bossche D. The A380 flight control electrohydrostatic actuators, achievements and lessons learnt. *25th International congress of the aeronautical sciences*; 2006 Sep 3–8; Hamburg, Germany. New York: Curran Associates Inc.; 2006. p. 3383–90.
2. MarÉ J-C, Fu J. Review on signal-by-wire and power-by-wire actuation for more electric aircraft. *Chin J Aeronaut* 2017;**30**(3):857–70.
3. Naayagi RT. A review of more electric aircraft technology. In International conference on energy efficient technologies for sustainability; 2013 April 10–12; Nagercoil, India. Piscataway, NJ: IEEE Computer Society; 2013. p. 750–3.
4. Wang SP, Cui XY, Shi J, Tomovic MM, Jiao ZX. Modeling of reliability and performance assessment of a dissimilar redundancy actuation system with failure monitoring. *Chin J Aeronaut* 2016;**29**(3):799–813.
5. Anderson EH, Lindler JE, Regelbrugge ME. Smart material actuator with long stroke and high power output. *43rd AIAA/ASME/ASCE/AHS/ASC structures, structural dynamics, and materials conference*; 2002 April 22–25; Denver, US. Reston, VA: AIAA Inc.; 2002.
6. Lindler JE, Anderson EH, Regelbrugge ME. Design and testing of piezoelectric-hydraulic actuators. *Smart structures and materials 2003: industrial and commercial applications of smart structures technologies*; 2003 March 4–6; San Diego, US. Bellingham, WA: SPIE; 2003. p. 96–107.
7. Jänker P, Claeyssen F, Grohmann B, Christmann M, Lorkowski T, LeLetty R, et al. New actuators for aircraft and space applications. *11th International conference on new actuators*; 2008 June 9–11; Bremen, Germany. Bremen: ACTUATOR Interest Group; 2008 p. 325–30.
8. Zhang R, Jiao ZX, Yan L, Wu S, Liang HS, Zheng JL. Design and numerical simulation of a continuable and bidirectional piezo-hydraulic servo pump. *2011 International conference on fluid power and mechatronics*; 2011 August 17–20; Beijing China. Piscataway, NJ: IEEE Computer Society; 2011 p. 498–504.
9. Kang RJ, Jiao ZX, Wang SP, Chen LS. Design and simulation of electro-hydrostatic actuator with a built-in power regulator. *Chin J Aeronaut* 2009;**22**(6):700–6.
10. Li Y, Jiao ZX, Yan L, Dong WH. Conceptual design and composition principles analysis of a novel collaborative rectification structure pump. *J Dyn Syst Meas Control Trans ASME* 2014;**136(5)**:054507–054507-8.
11. Nystad BH, Gola G, Hulsund JE, Roverso D. Technical condition assessment and remaining useful life estimation of choke valves subject to erosion. *Annual conference of the prognostics and health management society*; 2010 October 13–16; Portland, OR, US. College Park, MD: Prognostics and Health Management Society; 2010. p. 11–3.
12. Zhang K, Yao JY, Jiang TM. Degradation assessment and life prediction of electro-hydraulic servo valve under erosion wear. *Eng Fail Anal* 2014;**36**(1):284–300.

13. Fang X, Yao JY, Yin XZ, Chen X, Zhang CH. Physics-of-failure models of erosion wear in electrohydraulic servovalve, and erosion wear life prediction method. *Mechatronics* 2013;**23**(8):1202–14.
14. Zhang XL, Chen XF, Li B, He ZJ. Review of life prediction for mechanical major equipments. *J Mech Eng* 2011;**47**(11):100–16.
15. Fitch EC, Hong IT. *Hydraulic system design for service assurance*. Stillwater, OK: BarDyne Inc.; 2004. p. 125–78.
16. Vaughan ND, Pomeroy PE, Tilley DG. The contribution of erosive wear to the performance degradation of sliding spool servovalves. *Proc Inst Mech Eng Part J: J Eng Tribol* 1998;**212**(6):437–51.
17. Yang YJ, Peng WW, Meng DB, Zhu SP, Huang HZ. Reliability analysis of direct drive electrohydraulic servo valves based on a wear degradation process and individual differences. *Proc Inst Mech Eng Part O: J Risk Reliab 2014*;**228(6)**:621–30.
18. Frawley P, Corish J, Niven A, Geron M. Combination of CFD and DOE to analyse solid particle erosion in elbows. *Int J Comput Fluid Dyn* 2009;**23**(5):411–26.
19. Tang P, Yang J, Zheng JY, Wong I, He SZ, Ye JJ, et al. Failure analysis and prediction of pipes due to the interaction between multiphase flow and structure. *Eng Fail Anal* 2009;**16**(5):1749–56.
20. El-Behery SM, Hamed MH, Ibrahim KA, El-Kadi MA. CFD evaluation of solid particles erosion in curved ducts. *J Fluids Eng Trans ASME* 2010;**132**(7):071303.
21. Finnie I. Some observations on the erosion of ductile metals. *Wear* 1972;**19**(1):81–90.
22. Tilly GP. A two stage mechanism of ductile erosion. *Wear* 1973;**23**(1):87–96.
23. Edwards JK. *Development, validation, and application of a three-dimensional, CFD-based erosion prediction procedure [dissertation]*. Tulsa (OK): The University of Tulsa; 2001.
24. Li Y, Wang SP, Shi J, Tomovic MM. Dynamic contaminated particles concentration-based degradation model of linear electro-hydrostatic actuator. *2017 Annual reliability and maintainability symposium*; 2017 January 23–26; Orlando, FL, US. Piscataway, NJ: IEEE Inc.; 2017.
25. Pan XD, Wang GL, Lu ZS, Liu ZH. Simulation research on effect of diametral clearance of spool valve to valve orifice discharge characteristic. *Key Eng Mater* 2009;**392–394**:184–8.
26. Zhang H, Xiong SP, Liang YW, Xiong XY. Analyses of erosion wear characteristic and structure research on hydraulic valve. *J China Coal Soc* 2008;**33**(2):214–7.
27. Haider A, Levenspiel O. Drag coefficient and terminal velocity of spherical and nonspherical particles. *Powder Technol* 1989;**58**(1):63–70.
28. Grant G, Tabakoff W. Erosion prediction in turbomachinery resulting from environmental solid particles. *J Aircr* 1975;**12**(5):471–8.
29. Forder A, Thew M, Harrison D. A numerical investigation of solid particle erosion experienced within oilfield control valves. *Wear* 1998;**216**(2):184–93.
30. Wallace MS, Dempster WM, Scanlon T, Peters J, McCulloch S. Prediction of impact erosion in valve geometries. *Wear* 2004;**256**(9–10):927–36.
31. Zhu HJ, Pan Q, Zhang WL, Feng G, Li X. CFD simulations of flow erosion and flow-induced deformation of needle valve: effects of operation, structure and fluid parameters. *Nucl Eng Des* 2014;**273**(1):396–411.